Experimental Investigation of the Effects of Geometry on the Performance Characteristics of the Disk-shaped Pressure Gain Combustor

Peng Hwee Chua, Avion Lim, Zhen Wei Teo, Xin Huang, Jiun-Ming Li, Chiang Juay Teo, Boo Cheong Khoo
National University of Singapore
Singapore

1 Introduction

Continuous pressure gain combustion (PGC) has garnered significant attention in recent years due to its potential to enhance efficiency and reduce the size of combustion systems. While extensive research has focused on annular PGCs, alternative designs such as linear Shuttling Transverse Combustors and Disk PGCs have emerged, albeit with less attention. Various research works (e.g., [2, 8]) have attempted to demonstrate positive pressure gain, defined as the ratio of total pressure at the combustor exit to the oxidiser inlet plenum. While numerical simulations predict gains of up to 70% [1], annular PGC experiments have yielded only marginal positive gains, with discrepancies attributed to non-idealities such as viscous and heat losses within the combustor.

The performance of pressure gain is influenced by geometrical factors, including nozzle choking and the nozzle-to-inlet area ratio [2], which should ideally approach unity. Additionally, injector design is crucial; reducing injector losses correlates with increased pressure gain [3]. However, measuring total pressure in PGCs is challenging due to the high enthalpy and unsteady flow field. Direct measurement techniques, such as using Kiel probes, are limited by their short operational duration before thermal ablation [4], while indirect methods such as the Equivalent Available Pressure (EAP) [1] and NPS [3] methods have been employed to derive combustor exit total pressures.

Despite numerous studies on annular PGCs, there remains a research gap regarding the performance of disk PGCs, which are advantageous due to their compact axial design. Preliminary computational studies suggest that radially inward flowing disk PGCs exhibit improved detonation speeds and pressure gain performance [5]. Experimental data indicate that the detonation speed in these systems can reach approximately 91% of the Chapman-Jouguet (CJ) speed for a single rotating wave, surpassing the typical 60%–80% observed in annular PGCs [7].

Building on these promising preliminary results, this study aims to investigate pressure gain in disk PGCs and to identify key parameters affecting performance by employing similar indirect measurement techniques for total pressure assessment as those used in annular PGC research.

Correspondence to: penghwee.chua@u.nus.edu

2 Geometry & Instrumentation

A modular Disk PGC (Figure 1) was designed for parametric testing. The combustion chamber has an outer diameter of 200 mm and an inner diameter of 70 mm, with a naturally decreasing chamber area due to its straight combustor wall design. This configuration achieves a minimum area reduction by a factor of 0.725 before the flow turns towards the nozzle. Oxidiser is injected into the combustion chamber through an inlet slot, while fuel is injected via 120 sets of 1 mm injector holes arranged in a cross-flow configuration to enhance reactant mixing. The various components are illustrated in Figure 1.

The Disk PGC features interchangeable oxidizer injector slots, chamber widths, and nozzles, allowing for a range of injector-to-chamber ($\frac{A_{3.1}}{A_{3.2}}$) and nozzle-to-chamber ($\frac{A_8}{A_{3.2}}$) area ratios and providing flexibility in experimental configurations. In this set of experiments, two oxidizer slot widths of 0.5 mm and 2.8 mm, two chamber widths of 13 mm and 18 mm, and various converging nozzles with outer diameters varying between 79 mm and 122.4 mm were tested. For the small oxidiser slot size of 0.5mm, a 0.45 mm feeler gauge was used to check the slot holes to ensure the evenness of the oxidiser slots.

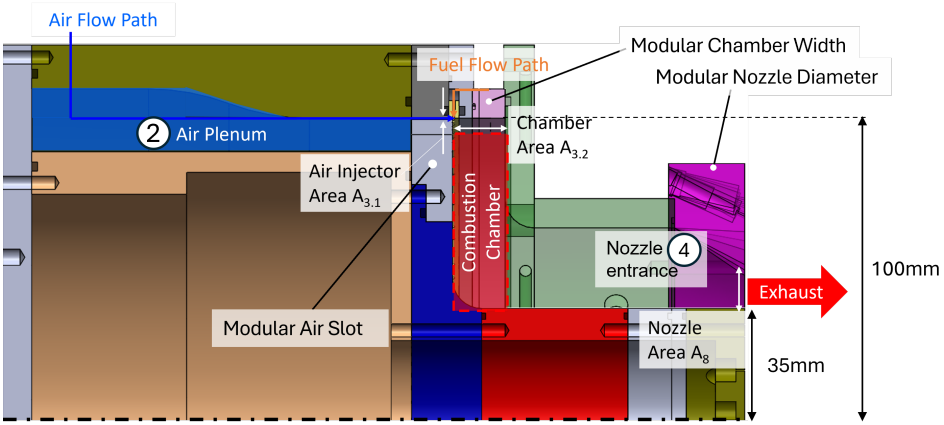

Figure 1: Map of possible area ratios

To measure static pressure within the air plenum, a physical plenum is fabricated. Given the expected slow flow conditions, static pressure is assumed to be approximately equal to the total pressure, serving as the denominator for the Pressure Gain calculations. For regions with expected high temperature flow, low-speed pressure transducers are arranged in a Capillary Tube Attenuated Pressure (CTAP) configuration, providing a standoff distance to prevent thermal damage to the transducers. One pressure transducer measures the average chamber pressure, and four pressure transducers, equally spaced azimuthally, measure 20 mm upstream of the nozzle entrance to account for azimuthal non-uniformity. Average values from the nozzle transducers are applied to derive the stagnation pressure at the combustor exit using the NPS methodologiesAverage values from the nozzle transducers are applied to derive the stagnation pressure at the combustor exit using the NPS methodologies [3,9]. Additionally, ten low-speed pressure transducers — seven on the centerbody base and three on the nozzle base — arranged in the CTAP configuration will measure base pressures near the exhaust. The Disk PGC will be mounted on a thrust stand equipped with an ATI-9105-TIF-GAMMA load cell for thrust measurement during experiments. Stagnation pressure at the combustor exit will also be calculated using the EAP methodology [1, 9], allowing for comparative analysis of results from both NPS and EAP methodologies. A high-speed camera was used to capture a portion of the flame luminosity within the chamber through the nozzle exit, allowing for wave modal analysis by correlating data with the high-frequency pressure transducer. The images represent flame luminosity in the visible light wavelength based on the spectral response of the camera, as no optical filter was used.

All low-speed pressure transducers arranged in the CTAP configuration for measuring averaged pressures in the chamber, nozzle, and base utilise STS ATM.1ST pressure transducers. Fuel plenum pressure is measured with an Omega PX429-100AI transducer, while air plenum pressure is measured using both an Omega PX429-250AI and an STS ATM.1ST transducer. Furthermore, two high-speed dynamic pressure transducers (PCB 113B24) capture the rapid pressure fluctuations within the chamber. Low-speed pressure transducer and load cell measurements were sampled at 1 kHz, while high-speed dynamic pressure transducer measurements were sampled at 500 kHz. The Photron SA-Z high-speed camera records at 40,000 frames per second with a shutter speed of 24 μs.

3 Experimental Results

This study investigates the effects of inlet width, chamber width, and nozzle width on the detonability and performance of a Disk Pressure Gain Combustor (PGC). The Disk PGC was operated for 1 second using gaseous air and ethylene across various geometric configurations, mass flow rates, and equivalence ratios. The nominal air mass flow rates ranged from 0.15 kg/s to 0.37 kg/s. An equivalence ratio sweep was conducted for each geometric configuration to investigate the lean and rich limits for sustained continuous detonation within the combustor. Equivalence ratios above 0.7 could not be tested at air mass flow rates exceeding 0.3 kg/s. Despite this, trends were observed in the results.

The experiment used two air slot widths (0.5 mm and 2.8 mm) and two chamber widths (18 mm and 13 mm). Converging nozzles were selected to achieve a nozzle-to-chamber area ratio ($\frac{A_8}{A_{3.2}}$) between 0.5 and 0.7, and an even smaller nozzle exit area was tested to choke the exit flow. An overview of the various testing conditions and the dominant wave mode is summarised in Figure 2.

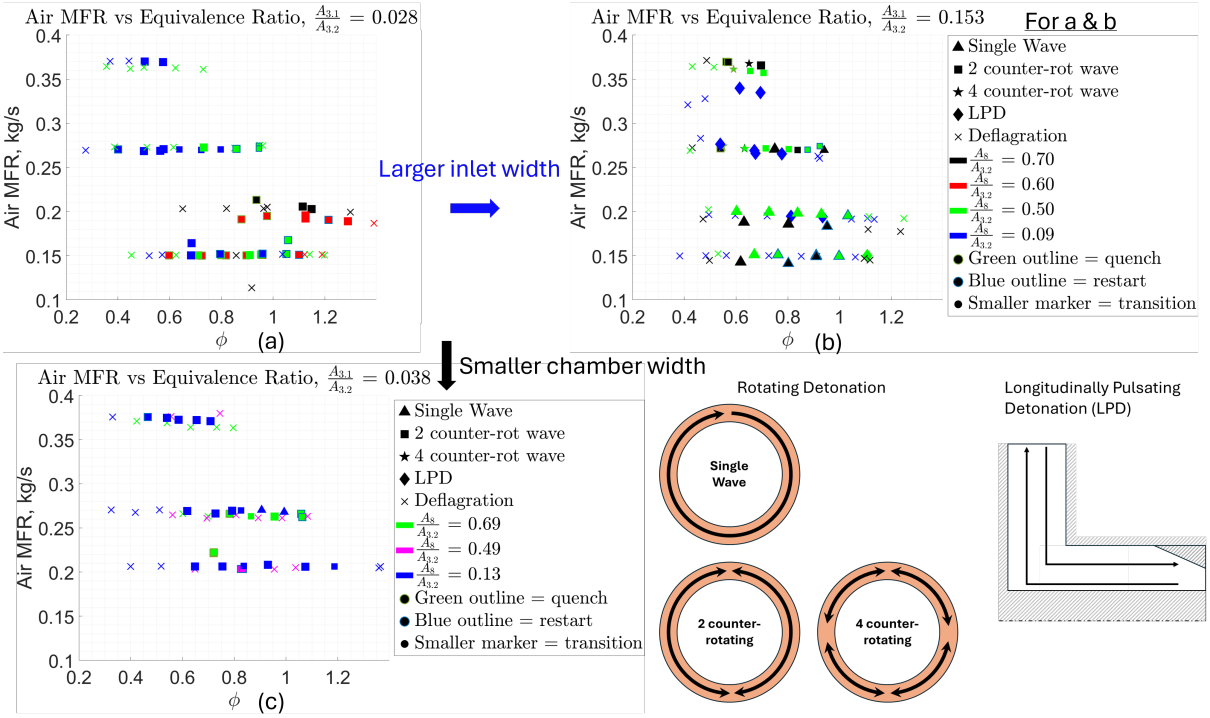

Figure 2: Test cases (a) Air Slot Width = 0.5mm, Chamber Width = 18mm, (b) Air Slot Width = 2.8mm, Chamber Width = 18mm, (c) Air Slot Width = 0.5mm, Chamber Width = 13mm

3.1 Detonation mode with Disk PGC

Various wave modes were identified during testing, including modal transitions, quenching events, and detonation wave re-establishment (restart) within the short firing duration. The dominant operational wave mode during operation has been characterised through analysis using multiple diagnostic methods: Short-Time Fourier Transform (STFT) of high-speed pressure transducer data, high-speed camera imaging, and a modified circuit wave analysis technique.

As shown in Figure 2, unstable detonation modes (quenching, restarting and modal transition) occur near the rich/lean limits where continuous detonation is marginally stable. These transitions could be driven by localised equivalence ratio fluctuations under near-critical conditions. As the global equivalence ratio is adjusted towards optimal chamber conditions, stable detonation modes are observed.

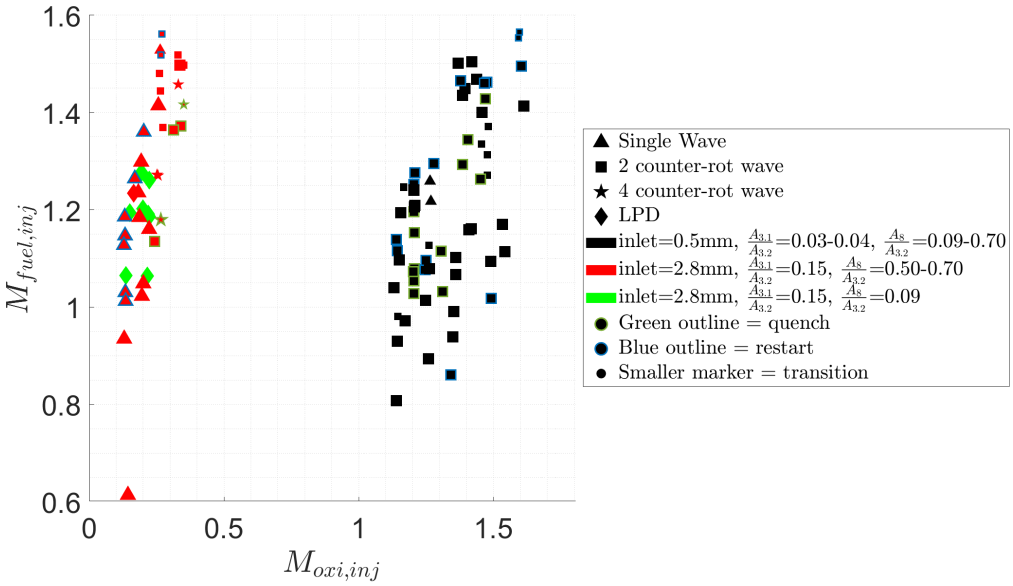

Figure 3: Fuel Inlet Mach Number vs Air Inlet Mach Number during pre-firing conditions

Oxidizer and fuel inlet Mach numbers were estimated using isentropic equations with plenum pressures and chamber pressures. While these calculated values are likely overestimates of the actual flow, they serve to understand the flow conditions at the injector. Figure 3 & Figure 4 presents these inlet Mach numbers plotted with pre-firing pressure results from -0.25s to -0.05s before ignition. From Figure 3, two counter-rotating waves dominate across configurations for 0.5mm air slots with higher air inlet Mach numbers. Increasing the air slot to 2.8 mm reduces air injection Mach numbers, and a single rotating wave dominates at lower fuel injector Mach numbers due to the insufficient reactant refill rate to sustain multiple detonation fronts. At higher air and fuel mass flow rates (Figure 2 & Figure 3), despite the small increase in air injection Mach number, multiple wave propagations (2 & 4 counter-rotating waves) emerge, suggesting an increased reactant available to sustain multiple waves.

Figure 5 indicates that the wave mode has the biggest influence on the detonation wave speed. The wave speed is normalised by the theoretical Chapman-Jouguet (CJ) detonation speed, calculated using the NASA CEA code [13]. Among the tested configurations, single wave mode achieved the highest wave speeds ranging from 1425 to 1610 m/s, corresponding to 79.2%-94.8% of the CJ detonation speed.Two counter-rotating waves exhibited lower speeds, with wave speeds bteween 1046 and 1547 m/s (62.1%-90.4% CJ speed), while four counter-rotating waves had the lowest wave speeds from 1058 to 1126 m/s

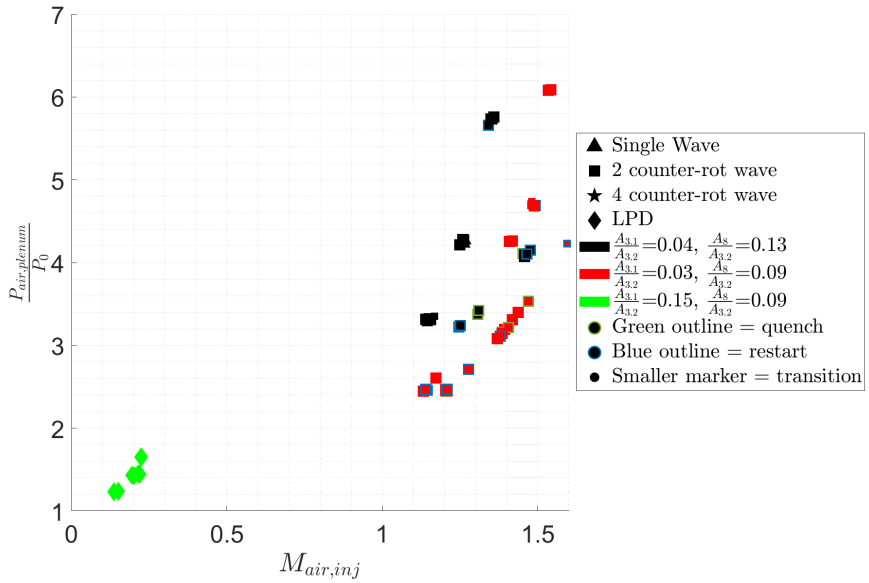

Figure 4: Normalised Air Plenum Pressure vs Air Inlet Mach Number of pre-firing conditions for nozzle diameter = 79mm

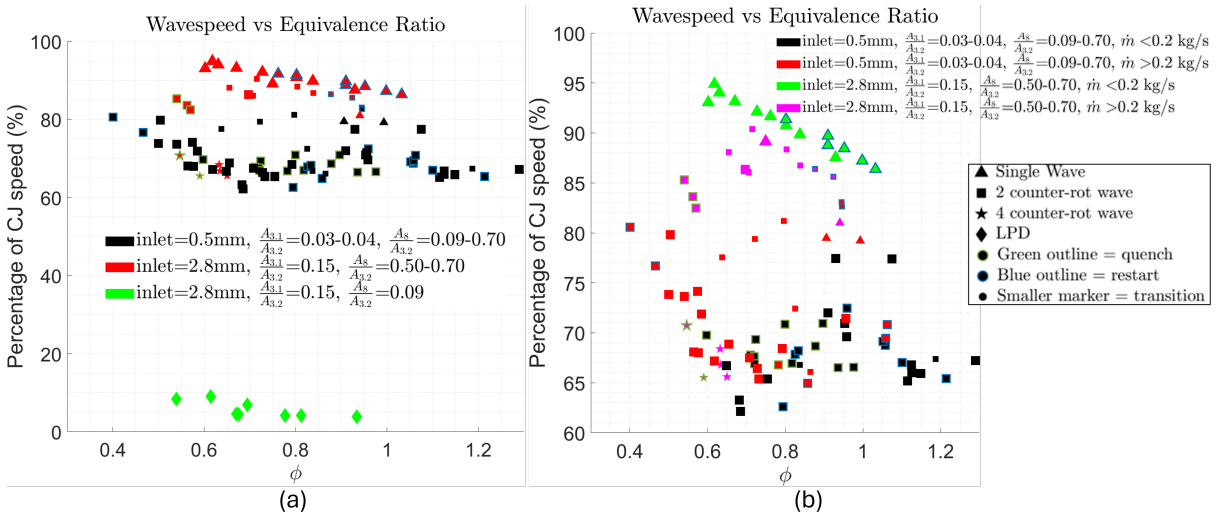

Figure 5: Wave Speed (as a % of CJ speed) vs equivalence ratio (a) for all test configurations & (b) for rotating detonation only

(65.5%-70.7% CJ speed). An increase in the number of waves reduces wave fill height and mixing time, reducing the strength and speed of the detonation waves.

Furthermore, an increase in mass flow rates appears to increase the wave propagation speed, as evidenced by the comparison between the red and black clusters in Figure 5b. For the same wave mode, higher reactant mass flow rates promote improved reactant mixing prior to the onset of detonation, resulting in a stronger detonation wave and higher wave velocity. This trend is consistent with findings for annular PGCs [14].

As shown in Figure 2a, the longitudinal pulsed detonation (LPD) mode was observed across all tested mass flow rates with area ratios $\frac{A_{3,1}}{A_{3,2}} = 0.153$ & $\frac{A_8}{A_{3,2}} = 0.09$, which correspond to the largest air slot width

and smallest nozzle area tested in this study. The wave speed during LPD mode was significantly lower, ranging between 71 to 148m/s (3.9–9.0% CJ speed), as indicated by pressure peaks recorded by high-speed pressure transducers. In contrast, two counter-rotating waves was observed when the air slot width is reduced while using the same nozzle configuration. As illustrated in Figure 4, while a smaller nozzle increases the backpressure effect and chamber pressure, the reduced pressure differential across the larger air slot resulted in a smaller injector Mach number, slowing the refill time. This condition inhibits the sustainment of high-frequency continuous rotating detonation, but creates suitable conditions for the occurrence of low-frequency longitudinal pulse detonation within the chamber.

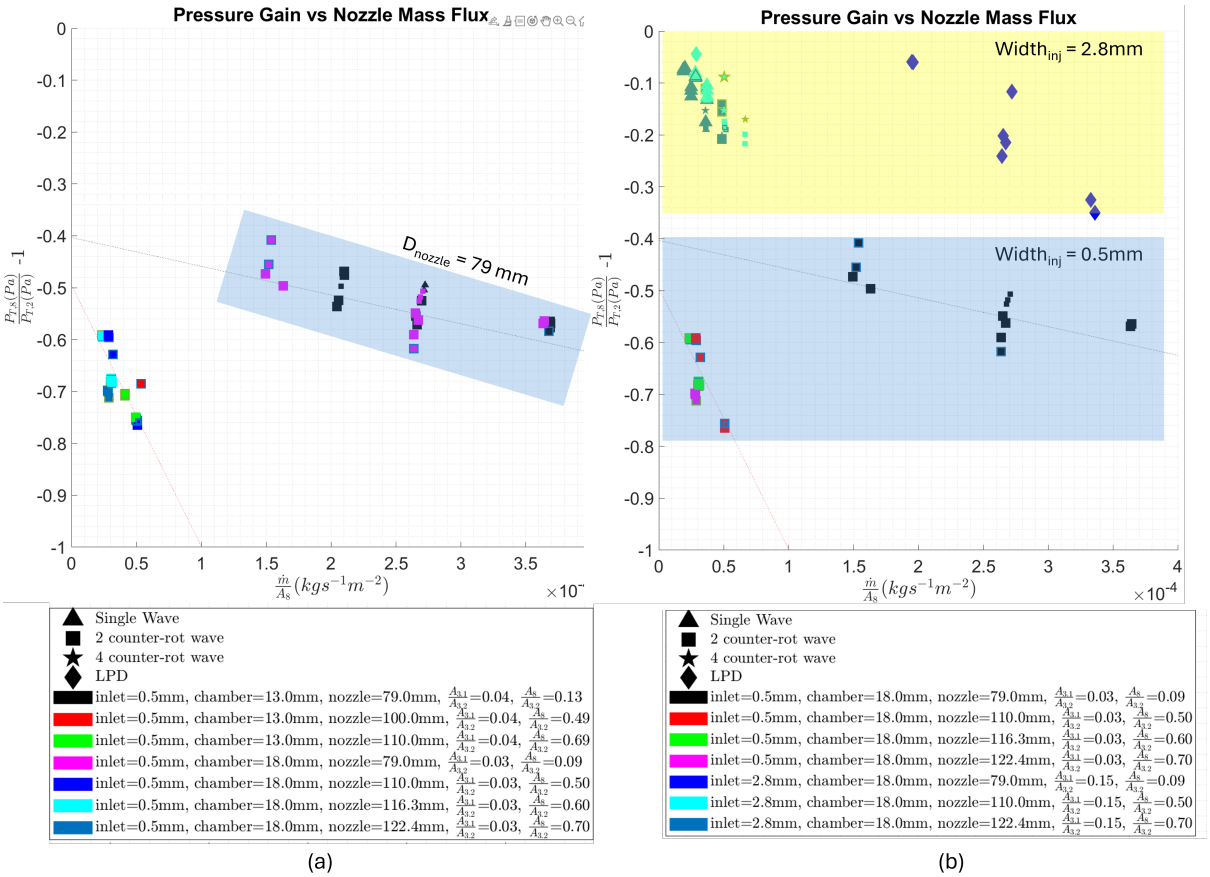

Figure 6: Effects of pressure gain due to change in (a) chamber width & (b) air slot width

3.2 Effects of Nozzle Diameter

Decreasing the nozzle area led to increased backpressure within the Disk PGC, resulting in higher chamber pressure and a reduced pressure ratio across the air plenum. This, in turn, slowed the reactant flow through both the air slot and fuel inlet, reducing viscous losses across the air slot, enhancing the pressure gain performance (defined as $\frac{P_{T,8}}{P_{T,2}}$ - 1) as illustrated in Figure 6.

An improvement in pressure gain was observed when $\frac{A_8}{A_{3.2}}$ was reduced from 0.7 to 0.5. For a chamber width of 18 mm, pressure gain improved from -71.2% to -69.1%, and for a chamber width of 13 mm, from -75.6% to -68.5%, at similar nozzle mass fluxes (Figure 6a). A comparable increase is also observed in Figure 6b, where pressure gain improved from -17.6% to -10.4%. Further reduction of the nozzle diameter to 79 mm ($\frac{A_8}{A_{3.2}}$ = 0.09 & 0.13) resulted in an improvement of pressure gain and a

significant increase in nozzle mass flux due to the smaller nozzle area.

3.3 Effects of Chamber Width

Increasing the channel width is generally believed to mitigate heat losses through the chamber walls and improve pressure gain [3, 8]. However, the present results indicated similar pressure gain across comparable area ratios ($\frac{A_{3.1}}{A_{3.2}}$ and $\frac{A_8}{A_{3.2}}$) and nozzle mass fluxes. As shown in Figure 6, linear trend lines indicate a weak dependency of pressure gain on chamber width, but a stronger linear relationship with the nozzle mass flux.

A distinct trend line describes the pressure gain when the nozzle diameter is reduced to 79 mm, likely because the nozzle is choked at most tested mass flow rates, whereas larger nozzles operate at low subsonic exit flow. Additionally, a smaller chamber width may adverse affect detonability in the Disk PGC (refer to Figure 2c), especially with larger nozzle diameters. This reduced detonability may be attributed to the detonation cell width of air-ethylene mixture being approximately 20mm [11] at atmospheric pressure. Consequently, higher chamber pressures are necessary to initiate detonation in chambers with chamber width of 13mm.

3.4 Effects of Inlet Width

Increasing the inlet width reduces viscous losses by reducing flow speed across the inlet, which leads to significant improvements in pressure gain, as shown in Figure 6b. Pressure gain ranges from -76.4% to -59.1% for air slot width of 0.5mm and from -21.7% to -4.1% for air slot width of 2.8 mm at the same $\frac{A_8}{A_{3.2}}$. However, larger inlets are more susceptible to backflow due to smaller pressure differentials across the inlet, which can limit the detonability range of the Disk PGC.

3.5 Comparison of methods used for pressure gain calculation

To evaluate the pressure gain performance of the Disk PGC, both the NPS and EAP methodologies were employed to derive the total pressure at the nozzle exit. Figure 7 presents a comparison of the total pressure values derived using the two approaches.

At lower mass flow rates, the nozzle exit flow remains unchoked for larger nozzle area ratios (A8/A3.2 = 0.49 -0.6), which corresponds to the clusters of data points on the left side of Figure 7. In these cases, the predicted total pressure is generally close to atmospheric pressure. As the nozzle throat area decreases, higher nozzle exit flow is achieved, and choked conditions are observed in some cases. These cases correspond to a higher total pressure derived from both methods.

Overall, the total pressure values derived from both approaches show good agreement for both deflagration and rotating detonation cases, as evidenced by the data points closely following the unity line. This consistency between methods is in line with similar findings reported for annular RDC [12].

4 Conclusion

This study systematically investigated the effects of varying inlet widths, chamber widths, and nozzle diameters on the performance of a Disk PGC across a range of mass flow rates from 0.15 to 0.37 kg/s using interchangeable configurations. The impact of the geometric parameters on pressure gain in the Disk PGC was quantified, and the dominant wave modes within the system were characterised.

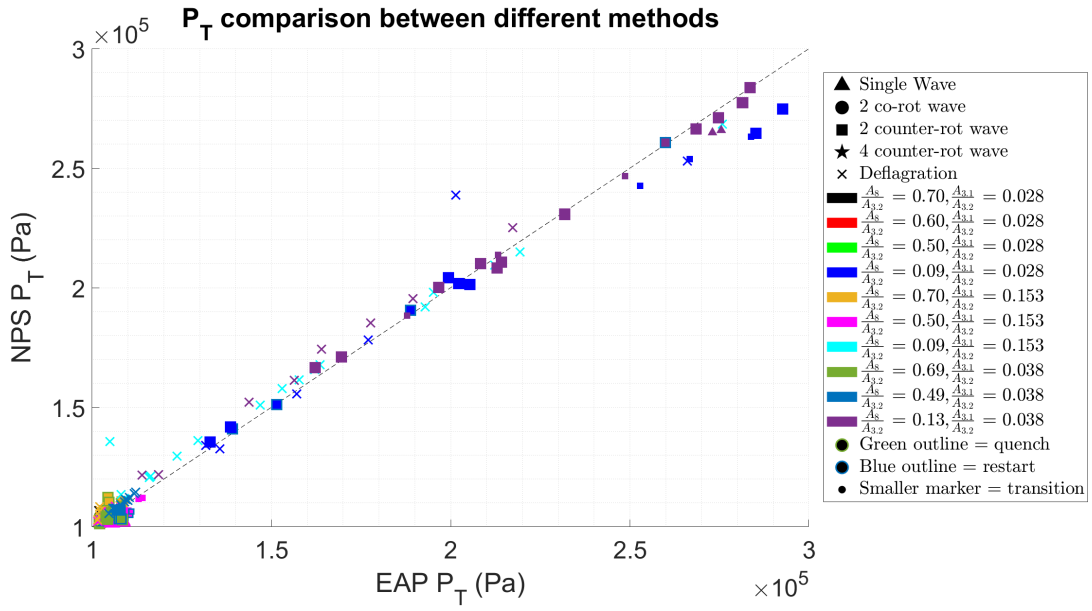

Figure 7: Wave Speed (as a % of CJ speed) vs equivalence ratio (a) for all test configurations & (b) for rotating detonation only

Consistent with previous results for Annular PGCs, configurations with larger injectors and smaller nozzles yielded higher pressure gains. Furthermore, total pressure values derived from both NPS and EAP methodologies showed good agreement for both deflagration and rotating detonation operation.

References

[1] Kaemming, T. A., D. E. Paxson (2018). Determining the pressure gain of pressure gain combustion. 2018 Joint propulsion conference.

[2] Bach, E., C. O. Paschereit, P. Stathopoulos, M. Bohon (2020). RDC operation and performance with varying air injector pressure loss. AIAA SciTech 2020 Forum.

[3] Brophy, C. M., Codoni, J. R., Thoeny, A. (2022). Channel Width Impact on RDE Performance with Fuel Injection Parity AIAA SCITECH 2022 Forum.

[4] Bach, E., Bohon, M., Paschereit, C. O., Stathopoulos, P. (2018). Development of an instrumented guide vane set for RDC exhaust flow characterization. 2018 Joint Propulsion Conference.

[5] Paxson, D. E. (2020). Preliminary computational assessment of disk rotating detonation engine configurations. AIAA Scitech 2020 Forum.

[6] Huang, X., Chang, P.-H., Li, J.-M., Juay Teo, C., Cheong Khoo, B. (2023). Operation and Power Generation of a Disk-Shaped Pressure Gain Combustor. Journal of Propulsion and Power, 39(6), 920-935.

[7] Raman, V., Prakash, S., Gamba, M. (2023). Nonidealities in rotating detonation engines. Annual Review of Fluid Mechanics, 55, 639-674.

[8] Brophy, C. M., Thoeny, A. (2024). Geometry Impact on the Operability and Delivered Pressure Gain Characteristics of a Rotating Detonation Combustor. AIAA SCITECH 2024 Forum.

[9] Fievisohn, R. T., Hoke, J., Holley, A. T. (2022). Experimental Measurements of Equivalent Available Pressure-Lessons Learned. AIAA SCITECH 2022 Forum.

[10] Chacon, F., Gamba, M. (2019). Detonation wave dynamics in a rotating detonation engine. AIAA Scitech 2019 Forum.

[11] Kaneshige, M., Shepherd, J. E. (1997). Detonation database. (California Institute of Technology)

[12] Bach, E., Thethy, B. S., Edgington-Mitchell, D., Rezay Haghdoost, M., Oliver Paschereit, C., Stathopoulos, P., ,Bohon, M. D. (2022). Kiel Probes for Stagnation Pressure Measurement in Rotating Detonation Combustors. AIAA Journal, 60(6), 3724-3735.

[13] Gordon, S., McBride, B. J. (1994). Computer program for calculation of complex chemical equilibrium compositions and applications. Part 1: Analysis

[14] Sato, T., Chacon, F., Gamba, M., Raman, V. (2021). Mass flow rate effect on a rotating detonation combustor with an axial air injection. Shock waves, 31(7), 741-751.